https://doi.org/10.15407/ujpe71.4.283

V.I. ROMANENKO, L.P. YATSENKO

Institute of Physics, Nat. Acad. of Sci. of Ukraine
(46, Nauky Ave., Kyiv 03028, Ukraine; e-mail: victor.romanenko@gmail.com)

BRAGG SCATTERING OF ATOMS BY COUNTER-PROPAGATING LIGHT PULSES ROBUST TO VARIATIONS OF PULSE AREAS

Bragg transitions of a two-level atom in the field of two pairs of counter-propagating light pulses with different carrier frequencies have been studied theoretically. Bragg transitions are treated as coherent multiphoton diffraction processes, in which, under an appropriate tuning to the Bragg resonance, the atomic momentum can change by $2n\hbar k$ *in a single scattering event, whereas single-photon transitions are suppressed due to a large detuning from the resonance. It has been shown that in this configuration, the transition efficiency is practically independent of the pulse area, in contrast to the case of a single pair of pulses. The physical basis of this effect consists in an almost adiabatic interaction of the atom with the field, similarly to the interaction with temporally overlapping counter-propagating pulses with off-resonant carrier frequencies [V.I. Romanenko, L.P. Yatsenko. Zh. Eksp. Teor. Fiz.* ***117****, 467 (2000); V.I. Romanenko, L.P. Yatsenko. JETP* ***90****, 407 (2000)]. The possibility of the momentum splitting of an atomic beam, which is robust with respect to variations of light intensity, and of the formation of selective laser mirrors has also been demonstrated. The proposed approach to control atomic motion can be applied to the study of interference phenomena in atomic optics.*

K e y w o r d s: atomic optics, laser radiation, Bragg transition, light pressure.

1. Introduction

Modern atomic optics and interferometry are based on the ability to control the internal state and the mechanical motion of an atom as a whole using coherent laser radiation. Among the methods for controlling the internal state and the mechanical motion, approaches based on the adiabatic interaction of an atom with an electromagnetic field occupy a special place, since they ensure the robustness of the result with respect to variations in interaction parameters. The fast adiabatic passage through resonance [1] became one of the first examples of adiabatic interaction between an atom and electromagnetic radiation in quantum optics. In the two-level model, which has been analyzed in Ref. [1], the carrier frequency of a light pulse, during the time of its action, passes through a resonance with the atomic transition frequency rather quickly so that spontaneous emission and coherence relaxation do not have enough time to significantly affect the process, but, at the same time, rather slowly so that the resonance passage can be considered adiabatic. As a result, a population inversion between the atomic states occurs, and the momentum of the atom changes by one photon's momentum.

Later it was shown that even in the framework of the two-level model, a much larger momentum can be transferred to the atom, and the result remains robust with respect to variations in the pulse area if the atom is subjected to the action of a pair of counter-propagating pulses with a large area and fixed carrier frequencies, which are detuned from the resonance transition frequency in the atom [2].

In Ref. [3], a scheme combining two phenomena was proposed: the interaction between an atom and a pair of counter-propagating light pulses, and the fast resonance passage, when the carrier frequencies of both pulses change in time with a certain time shift between them (in contrast to the fixed carrier

C i t a t i o n: Romanenko V.I., Yatsenko L.P. Bragg scattering of atoms by counter-propagating light pulses robust to variations in their areas. *Ukr. J. Phys.* **71**, No. 4, 283 (2026). https://doi.org/10.15407/ujpe71.4.283.

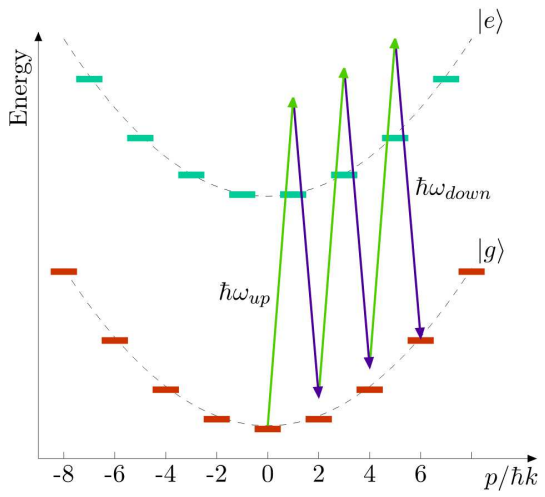

Fig. 1. Schematic diagram of a six-photon Bragg transition

frequencies considered in Ref. [2]). With an emphasis on the large momentum transfer to an atom that is robust to the change in the area of light pulses, Raman transitions in three-level atoms were also studied [4]. Since these transitions have a Raman character, two pairs of pulses were used; each of them induced its own Raman transition with two-photon detuning that differs for the different pairs.

Bragg transitions in atoms under the action of two counter-propagating light pulses with different carrier frequencies satisfying the resonance condition can be described as transitions between two atomic states with different momenta (see Fig. 1), which are coupled by a certain effective field characterized by a multiphoton Rabi frequency [5]. In the framework of this interaction scenario, a fast adiabatic passage of resonance can be realized, when the two-photon detuning changes rapidly within a certain interval [6]. In contrast to the fast adiabatic passage in a two-level atom, the destructive effect of spontaneous emission from the excited state is practically absent, since this state is almost depopulated. Another method of transferring a large momentum to an atom, which is insensitive to changes in the area of light pulses and related to the momentum transfer at the interaction of a two-level atom with two counter-propagating pulses with different carrier frequencies, has not been considered so far.

In this paper, a method of transferring a momentum of the order of several photon pulses to an atom (for $2n$-photon transitions, this is a momentum of $2n\hbar k$, where n is an integer, and k is the wave vector of the light waves), which is robust to changes in the area of light pulses, is proposed for Bragg transitions. This method, similarly to the partial fast resonance passage [6], makes it possible to split atomic waves and implement atomic mirrors.

The article is structured as follows. In the next section, main equations describing the behavior of an atom in a field of four pairwise counter-propagating light pulses with different frequencies are presented. In Section 3, a procedure of adiabatic elimination of the excited state is described. In Section 4, the results of numerical simulations of Bragg transitions in a four-pulse field are given. In Section 5, the main conclusions are formulated.

2. Basic Equations

Let a two-level atom (with the ground state $|g\rangle$ and the excited state $|e\rangle$) interacts with a field $\boldsymbol{E}$ of four light pulses: two of them (pulses 1 and 2) propagate along the z axis, and the other two (pulses 3 and 4) propagate in the opposite direction. Hence,

$$\boldsymbol{E} = E_1(t)\boldsymbol{e}_1\cos(\omega_1 t - k_1 z + \varphi_1) + \\ + E_2(t)\boldsymbol{e}_2\cos(\omega_2 t - k_2 z + \varphi_2) + \\ + E_3(t)\boldsymbol{e}_3\cos(\omega_3 t + k_3 z + \varphi_3) + \\ + E_4(t)\boldsymbol{e}_4\cos(\omega_4 t + k_4 z + \varphi_4),$$

where $\boldsymbol{e}_n$ $(n = 1, ..., 4)$ are the unit vectors of the electric field direction, $E_n(t)$ are the envelopes of the field strengths of the pulses, ω_n are the carrier frequencies of the pulses, k_n are the projections of the pulses' wave vectors onto the z-axis, and φ_n are the initial phases of the pulses. Since the difference between the carrier frequencies is much smaller than the atomic transition frequency, we will neglect below the difference among the wave vectors and assume that $k_1 = k_2 = k_3 = k_4 \equiv k$.

The dynamics of the atomic state vector $|\Psi\rangle$ is described by the Schrödinger equation

$$i\hbar\frac{\partial}{\partial t}|\Psi\rangle = (H_0 - \widehat{\boldsymbol{d}}\boldsymbol{E})|\Psi\rangle - i\hbar\frac{\gamma}{2}|e\rangle\langle e|\Psi\rangle. \qquad (1)$$

Here, H_0 is the free-atom Hamiltonian, $\widehat{\boldsymbol{d}}$ is the dipole moment operator, and γ is the spontaneous emission rate. This equation is equivalent to the equation for the density matrix if the atomic state is given by the Monte Carlo wave function [7, 8]. If we take the

ground state energy to equal zero, and the excited state energy to equal $\hbar\omega_0$, then the Hamiltonian H_0 of a free atom has the form

$$H_0 = \frac{\widehat{\boldsymbol{p}}^2}{2M} + \hbar\omega_0 |e\rangle\langle e|, \tag{2}$$

where $\widehat{\boldsymbol{p}}$ is the atomic momentum operator.

The wave function is a superposition of the ground and excited states, with the amplitudes varying in time and space,

$$|\Psi\rangle = c_e(z,t)e^{-i\omega_0 t}\,|e\rangle + c_g(z,t)\,|g\rangle\,. \tag{3}$$

The coefficients $c_g(z,t)$ and $c_e(z,t)$ are expanded in a series in the eigenfunctions $\langle z|n\rangle = \exp(inkz)$ of the z-component of the momentum operator, with the eigenvalues $n\hbar k$:

$$c_g = \sum_{n=-\infty}^{+\infty} b_{g,n}e^{i\alpha kz}\,\langle z\,|n\rangle\,, \tag{4a}$$

$$c_e = \sum_{n=-\infty}^{+\infty} b_{e,n}e^{i\alpha kz}\,\langle z\,|n\rangle\,. \tag{4b}$$

Here, α is the fractional part of the ratio between the initial atomic momentum and $\hbar k$. Below, to simplify numerical simulations, we consider the case $\alpha = 0$. The coefficients $b_{g,n}$ and $b_{e,n}$ in expansions (4) are the amplitudes of the probability for finding the atom in the states $|g\rangle$ or $|e\rangle$, respectively, with momentum $n\hbar k$. To simplify the notation in Eqs. (4) and below, we do not specify the arguments of c_g, c_e, $b_{g,n}$, and $b_{e,n}$.

Substituting Eqs. (4) into the Schrödinger equation (1), we obtain the following equations for $b_{g,n}$ and $b_{e,n}$:

$$\begin{aligned} i\frac{\partial}{\partial t}b_{g,n} &= \delta_{\rm rec}n^2 b_{g,n} + \frac{1}{2}\Omega_1 b_{e,n+1}e^{i\delta_1 t+i\varphi_1} + \\ &+ \frac{1}{2}\Omega_2 b_{e,n+1}e^{i\delta_2 t+i\varphi_2} + \frac{1}{2}\Omega_3 b_{e,n-1}e^{i\delta_3 t+i\varphi_3} + \\ &+ \frac{1}{2}\Omega_4 b_{e,n-1}e^{i\delta_4 t+i\varphi_4}, \end{aligned} \tag{5a}$$

$$\begin{aligned} i\frac{\partial}{\partial t}b_{e,n} &= \delta_{\rm rec}n^2 b_{e,n} - i\frac{\gamma}{2}b_{e,n} + \\ &+ \frac{1}{2}\Omega_1^* b_{g,n-1}e^{-i\delta_1 t-i\varphi_1} + \frac{1}{2}\Omega_2^* b_{g,n-1}e^{-i\delta_2 t-i\varphi_2} + \\ &+ \frac{1}{2}\Omega_3^* b_{g,n+1}e^{-i\delta_3 t-i\varphi_3} + \frac{1}{2}\Omega_4^* b_{g,n+1}e^{-i\delta_4 t-i\varphi_4}. \end{aligned} \tag{5b}$$

Here, we introduce the time-varying Rabi frequencies Ω_1, Ω_2, Ω_3 and Ω_4, which are determined by the formulas

$$\Omega_1 = -\frac{\langle g|\,\boldsymbol{de}_1\,|e\rangle\,E_1}{\hbar}\,, \quad \Omega_2 = -\frac{\langle g|\,\boldsymbol{de}_2\,|e\rangle\,E_2}{\hbar},$$
$$\Omega_3 = -\frac{\langle g|\,\boldsymbol{de}_1\,|e\rangle\,E_3}{\hbar}\,, \quad \Omega_4 = -\frac{\langle g|\,\boldsymbol{de}_2\,|e\rangle\,E_4}{\hbar},$$

as well as the notations $\delta_{\rm rec} = \hbar k^2/(2M)$ and $\delta_n = \omega_n - \omega_0$ $(n = 1,2,3,4)$. The terms oscillating with doubled carrier frequencies of light pulses are neglected (the rotating wave approximation [9]).

The time dependence of the amplitudes of light pulses is described by the expression

$$\Omega_n = \Omega_{n0}F_2\left(\frac{t}{\tau_n} - t_{dn}\right), \quad n = 1,2,3,4, \tag{6}$$

where τ_n is the n-th pulse duration, and t_{dn} is the time when the n-th pulse amplitude reaches maximum, counted from the initial time moment. The function $F_2(x)$ belongs to the sequence of functions

$$F_m(x) = \begin{cases} \cos^m\left(\pi x\sqrt{\dfrac{2}{m}}\right) & \text{for } |x| \le \sqrt{\dfrac{m}{8}}, \\ 0 & \text{for } |x| \ge \sqrt{\dfrac{m}{8}}, \end{cases} \tag{7}$$

which converges to $\exp(-\pi^2x^2)$ when $m \to \infty$ [10].

3. Adiabatic Switching-Off of Excited State

The general picture of interaction between a two-level atom and four incident light pulses is quite complicated. It is enough to list the parameters on which it depends: the durations of light pulses, the time shifts of light pulses with respect to the reference time, the initial phases of light pulses, the Rabi frequencies, the recoil energy, and the detuning of the carrier frequencies of light pulses from resonance with the atomic transition. Among the variety of phenomena taking place in the system "atom–field of four light pulses", only a phenomenon analogous to the momentum transfer at the interaction of a two-level atom with two counter-propagating pulses [2] is considered; the difference is that the focus is placed on Bragg transitions in which the excited atomic state remains practically depopulated.

Recall that in Ref. [2], it was shown the following. When an atom interacts with light pulses with different carrier frequencies, there arise step-like dependences of the momentum transmitted to the atom

on the Rabi frequency, and the average detuning of the pulses' carrier frequencies from the transition frequency in the atom. Those dependences are a result of quasi-adiabatic atom–field interaction in a rather wide intervals of parameter changes. A transition from one step to another is associated with the violation of adiabaticity, when the relative arrangement of adiabatic quasi-energies changes due to the changes in the interaction parameters of the atom–field system. Later, various aspects of this phenomenon were studied in detail in a number of works [3, 11–15].

When searching for an analogy to Bragg transitions, two-photon transitions are considered instead of single-photon ones, since they couple states with different momentum values in the same electronic state. The detuning from the single-photon resonance is large enough in this case for the excited atomic state to be practically depopulated. Thus, it is necessary to consider the interaction of an atom with two pairs of light pulses, each of which causes a two-photon transition in the atom. We will assume that such pairs are composed of pulses 1–3 and 2–4. It will also be assumed that the frequency differences between pulses 1 and 2 – and, therefore, between pairs 1–4, 2–3, and 3–4 – are so large that these combinations do not excite a two-photon transition.

The presence of rapidly oscillating multipliers in Eqs. (5) (these are exponents containing $\delta_j t$, $j = 1$, 2, 3, 4) substantially slows down the process of numerical solution of those equations. In order to speed it up, let us simplify Eqs. (5) using the assumption made above about a large detuning of the carrier frequencies of light pulses from the atomic transition frequency. The pairwise proximity of the frequencies δ_1, δ_3 and δ_2, δ_4 is mathematically written down as $\delta_1 \approx \delta_3 \approx \Delta_{13}$, $\delta_2 \approx \delta_4 \approx \Delta_{24}$, $|\delta_1 - \delta_3| \ll |\Delta_{13}|$, and $|\delta_2 - \delta_4| \ll |\Delta_{24}|$. Let us introduce the notation $\tilde{\delta}_1 = \delta_1 - \Delta_{13}$, $\tilde{\delta}_3 = \delta_3 - \Delta_{13}$, $\tilde{\delta}_2 = \delta_2 - \Delta_{24}$, and $\tilde{\delta}_4 = \delta_4 - \Delta_{24}$.

From the analysis of Eqs. (5), it follows that the amplitudes $b_{e,n}$ of the excited state oscillate with high frequencies of the order of Δ_{13} and Δ_{24}, whereas the amplitudes $b_{g,n}$ of the ground state contain a slowly varying component and components oscillating with the frequencies $2\Delta_{13}$ and $2\Delta_{24}$. Below, in the amplitudes $b_{g,n}$, we neglect the terms oscillating with these frequencies (the rotating wave approximation [9]), as well as the terms oscillating with the frequencies $|\Delta_{13} \pm \Delta_{24}|$. Thus, the amplitudes $b_{e,n}$ are sought in the form

$$b_{e,n} = b_{e,n}^{(13)} e^{-i\Delta_{13}t} + b_{e,n}^{(24)} e^{-i\Delta_{24}t}, \tag{8}$$

where the factors $b_{e,n}^{(13)}$ and $b_{e,n}^{(24)}$ change slowly in time. As a result, Eqs. (5) take the following form:

$$i\frac{\partial}{\partial t} b_{g,n} = \delta_{\rm rec} n^2 b_{g,n} + \frac{1}{2}\Omega_1 b_{e,n+1}^{(13)} e^{i\tilde{\delta}_1 t + i\varphi_1} + \\ + \frac{1}{2}\Omega_2 b_{e,n+1}^{(24)} e^{i\tilde{\delta}_2 t + i\varphi_2} + \frac{1}{2}\Omega_3 b_{e,n-1}^{(13)} e^{i\tilde{\delta}_3 t + i\varphi_3} + \\ + \frac{1}{2}\Omega_4 b_{e,n-1}^{(24)} e^{i\tilde{\delta}_4 t + i\varphi_4}, \tag{9a}$$

$$i\frac{\partial}{\partial t} b_{e,n}^{(13)} = \delta_{\rm rec} n^2 b_{e,n}^{(13)} - \left(\Delta_{13} + i\frac{\gamma}{2}\right) b_{e,n}^{(13)} + \\ + \frac{1}{2}\Omega_1^* b_{g,n-1} e^{-i\tilde{\delta}_1 t - i\varphi_1} + \frac{1}{2}\Omega_3^* b_{g,n+1} e^{-i\tilde{\delta}_3 t - i\varphi_3}. \tag{9b}$$

$$i\frac{\partial}{\partial t} b_{e,n}^{(24)} = \delta_{\rm rec} n^2 b_{e,n}^{(24)} - \left(\Delta_{24} + i\frac{\gamma}{2}\right) b_{e,n}^{(24)} + \\ + \frac{1}{2}\Omega_2^* b_{g,n-1} e^{-i\tilde{\delta}_2 t - i\varphi_2} + \frac{1}{2}\Omega_4^* b_{g,n+1} e^{-i\tilde{\delta}_4 t - i\varphi_4}. \tag{9c}$$

The derivatives $\frac{\partial}{\partial t} b_{e,n}^{(13)}$ and $\frac{\partial}{\partial t} b_{e,n}^{(24)}$ are small in comparison with the quantities $\Delta_{13} b_{e,n}^{(13)}$ and $\Delta_{24} b_{e,n}^{(24)}$, respectively, so we will neglect them below. In addition, the rate of spontaneous emission is also low in comparison with Δ_{13} and Δ_{24}, and we will also neglect it, bearing in mind that the influence of spontaneous emission on the time evolution of wave function is insignificant under the condition

$$\gamma\tau \max\left(|b_{e,n}^{(13)}|^2\right) \ll 1, \quad \gamma\tau \max\left(|b_{e,n}^{(24)}|^2\right) \ll 1. \tag{10}$$

To be consist with the approximation made above, we also neglect the term $\delta_{\rm rec} n^2 \tilde{b}_{e,n}$, associated with the recoil effect, in Eqs. (9b) and (9c). As a result, we obtain

$$b_{e,n}^{(13)} = \frac{\Omega_1^*}{2\Delta_{13}} b_{g,n-1} e^{-i\tilde{\delta}_1 t - i\varphi_1} + \\ + \frac{\Omega_3^*}{2\Delta_{13}} b_{g,n+1} e^{-i\tilde{\delta}_3 t - i\varphi_3}, \tag{11}$$

$$b_{e,n}^{(24)} = \frac{\Omega_2^*}{2\Delta_{24}} b_{g,n-1} e^{-i\tilde{\delta}_2 t - i\varphi_2} + \\ + \frac{\Omega_4^*}{2\Delta_{24}} b_{g,n+1} e^{-i\tilde{\delta}_4 t - i\varphi_4}. \tag{12}$$

As follows from Eqs. (9), the phases of complex Rabi frequencies can be included into the phases φ_n

($n = 1, 2, 3, 4$) of the electric field. Therefore, in what follows, we will consider the Rabi frequencies to be real quantities without loss of generality.

Substituting Eqs. (11) and (12) into Eq. (9a), we obtain a chain of equations for the population amplitudes of ground state with different momenta,

$$i\frac{\partial}{\partial t}b_{g,n} = \left(\delta_{\rm rec}n^2 + \frac{\Omega_1^2}{4\Delta_{13}} + \frac{\Omega_2^2}{4\Delta_{24}} + \right.$$
$$\left. + \frac{\Omega_3^2}{4\Delta_{13}} + \frac{\Omega_4^2}{4\Delta_{24}}\right) b_{g,n} +$$
$$+ \left(\frac{\Omega_1\Omega_3}{4\Delta_{13}}e^{i\Phi_{13}} + \frac{\Omega_2\Omega_4}{4\Delta_{24}}e^{i\Phi_{24}}\right) b_{g,n+2} +$$
$$+ \left(\frac{\Omega_1\Omega_3}{4\Delta_{13}}e^{-i\Phi_{13}} + \frac{\Omega_2\Omega_4}{4\Delta_{24}}e^{-i\Phi_{24}}\right) b_{g,n-2}. \quad (13)$$

Here,

$$\Phi_{13} = (\tilde{\delta}_1 - \tilde{\delta}_3)t + \varphi_1 - \varphi_3,$$
$$\Phi_{24} = (\tilde{\delta}_2 - \tilde{\delta}_4)t + \varphi_2 - \varphi_4, \quad (14)$$

Let us introduce the quantities

$$R_1 = \frac{\Omega_1^2}{2\Delta_{13}}, \quad R_2 = \frac{\Omega_2^2}{2\Delta_{24}},$$
$$R_3 = \frac{\Omega_3^2}{2\Delta_{13}}, \quad R_4 = \frac{\Omega_4^2}{2\Delta_{24}} \quad (15)$$

and change in the variables

$$B_n = b_{g,n}e^{\frac{1}{2}in\delta_0 t + \frac{1}{2}in\Phi}, \quad (16)$$

where

$$\delta_0 = \frac{1}{2}(\tilde{\delta}_1 - \tilde{\delta}_3 + \tilde{\delta}_2 - \tilde{\delta}_4) \quad (17)$$

is the average two-photon detuning, and

$$\Phi = \frac{1}{2}(\varphi_1 - \varphi_3 + \varphi_2 - \varphi_4). \quad (18)$$

Note that the quantities R_1, R_2, R_3, and R_4 can be either positive or negative depending on the signs of Δ_{13} and Δ_{24}. At the same time, the products R_1R_3 and R_2R_4 are always positive.

From Eqs. (13), we obtain the following equation for the quantities B_n:

$$\frac{\partial}{\partial t}B_n = -i\left(\delta_{\rm rec}n^2 - \frac{1}{2}n\delta_0 + \right.$$
$$\left. + \frac{R_1}{2} + \frac{R_2}{2} + \frac{R_3}{2} + \frac{R_4}{2}\right) B_n -$$
$$- i\left(\mathrm{sign}(\Delta_{13})\frac{\sqrt{R_1R_3}}{2}e^{-\frac{1}{2}i\delta t - \frac{1}{2}i\varphi} + \right.$$
$$\left. + \mathrm{sign}(\Delta_{24})\frac{\sqrt{R_2R_4}}{2}e^{\frac{1}{2}i\delta t + \frac{1}{2}i\varphi}\right) B_{n+2} -$$
$$- i\left(\mathrm{sign}(\Delta_{13})\frac{\sqrt{R_1R_3}}{2}e^{\frac{1}{2}i\delta t + \frac{1}{2}i\varphi} + \right.$$
$$\left. + \mathrm{sign}(\Delta_{24})\frac{\sqrt{R_2R_4}}{2}e^{-\frac{1}{2}i\delta t - \frac{1}{2}i\varphi}\right) B_{n-2}. \quad (19)$$

Here,

$$\delta = \tilde{\delta}_1 - \tilde{\delta}_3 - \tilde{\delta}_2 + \tilde{\delta}_4, \quad (20)$$

which corresponds to the difference between two-photon detunings, and

$$\varphi = \varphi_1 - \varphi_3 - \varphi_2 + \varphi_4. \quad (21)$$

From Eqs. (19), it is clear that the quantities $\sqrt{R_1R_3}$ and $\sqrt{R_2R_4}$ are two-photon Rabi frequencies, and they couple atomic states with the momenta that differ by $2\hbar k$.

4. Results of Numerical Calculations and Their Analysis

In this Section, we will use the idea that the atom is in an adiabatic state during most of the time of its interaction with the field as a basic guideline for understanding the results of numerical calculations.

4.1. Bragg transitions under the action of two light pulses

First of all, let us find a condition for $2n$-photon resonance, when an atom transits from the state with momentum $n_i\hbar k$ into the state with momentum $n_f\hbar k$ ($n_f = n_i + 2n$, where n_i and n_f are integers). To observe the Bragg resonance, two counter-propagating light pulses are sufficient in this case (to be more specific, let pulses 2 and 4 do not act on the atom). Then, after every two-photon transition with absorption of a photon from the field of pulse 1 and its emission into the field of pulse 3, the kinetic energy of the atom changes by $\hbar(\omega_1 - \omega_3) = \hbar(\tilde{\delta}_1 - \tilde{\delta}_3)$. For a $2n$-photon transition, we have

$$\hbar n(\tilde{\delta}_1 - \tilde{\delta}_3) = \hbar\delta_{\rm rec}(n_f^2 - n_i^2), \quad (22)$$

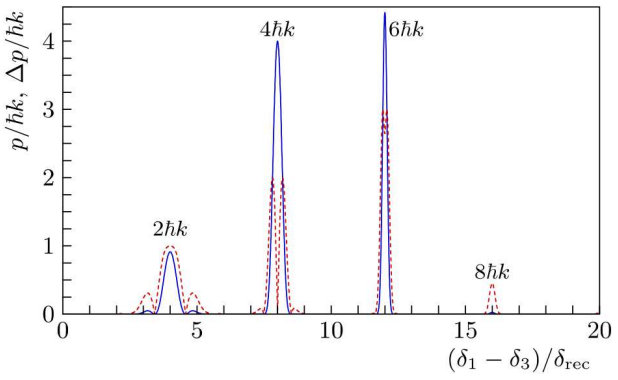

Fig. 2. Dependences of the average momentum p transmitted to the atom (solid curve) and its root-mean-square deviation Δp from the average value (dashed curve) on the carrier frequency difference $\delta_1 - \delta_3$ between pulses 1 and 3. Pulses 2 and 4 do not act on the atom. The maximum values of R_1 and R_3 are identical and equal to $R_0 = 4.316257\delta_{\rm rec}$; they were chosen so that the magnitude of the transmitted momentum in the four-photon process equals $4\hbar k$. The light pulses coincide in time; their duration is $10\pi/\delta_{\rm rec}$. At the beginning of its interaction with the field, the atom was in a state with zero momentum. The maxima of the momentum transferred to the atom and marked by $2\hbar k$, $4\hbar k$, $6\hbar k$, and $8\hbar k$ correspond to two-, four-, six-, and eight-photon Bragg transitions, respectively

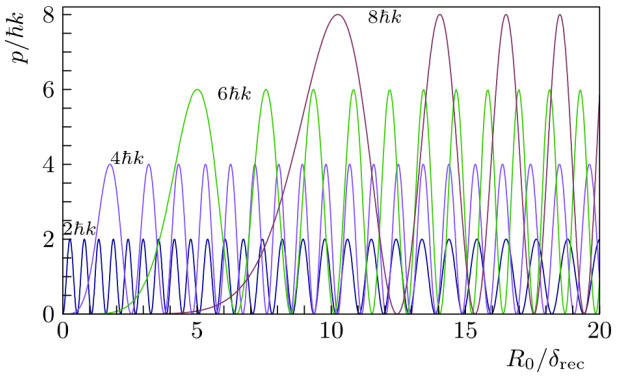

Fig. 3. Dependences of the average momentum transferred to the atom on the two-photon Rabi frequency for various carrier frequency differences. The atom is in a state with zero momentum. At the carrier frequency difference $\delta_1 - \delta_3 = 4\delta_{\rm rec}$, $8\delta_{\rm rec}$, , $12\delta_{\rm rec}$, or $16\delta_{\rm rec}$, Bragg transitions take place between the state with zero momentum and the state with momentum $2\hbar k$, $4\hbar k$, $6\hbar k$, or $8\hbar k$, respectively. Pulses 2 and 4 do not act on the atom. Light pulses 1 and 3 coincide in time; their duration is $10\pi/\delta_{\rm rec}$

which gives the resonance condition

$$\tilde{\delta}_1 - \tilde{\delta}_3 = 2\delta_{\rm rec}(n_f + n_i). \tag{23}$$

Positive n_i-values correspond to the motion of the atom in the positive direction of the OZ-axis, and negative ones in the negative direction. The same also concerns n_f.

For the initial state with zero momentum, two-, four-, six-, and eight-photon resonances take place at $\tilde{\delta}_1 - \tilde{\delta}_3 = 4\delta_{\rm rec}$, $8\delta_{\rm rec}$, $12\delta_{\rm rec}$, and $16\delta_{\rm rec}$, respectively; see Fig. 2). For the values of the parameters of interaction between the atom and the fields of pulses 1 and 3 that were chosen for calculations, the transferred momentum reaches the maximum value only in the case of four-photon transition because the multi-photon Rabi frequencies are different for the indicated transitions [5].

Figure 3 illustrates how the momentum transferred to the atom changes as the quantity R_0 (the maximum of the two-photon Rabi frequency, $\sqrt{R_1 R_3}$) varies in the cases of two-, four-, six-, and eight-photon transitions. The change of the atomic momentum reflects the change in the population of the atomic states with momenta $2\hbar k$, $4\hbar k$, $6\hbar k$, and $8\hbar k$ (if the atom has zero momentum in the initial state) according to the fact that at the Bragg resonance, with an accuracy to the population losses due to relaxation processes, a two-level scheme of interaction of the atom with the field of counter-propagating light pulses is formed [5]. As one can see, the robustness of transferred momentum to the change of R_0 is out of the question here. This robustness can be provided, for example, by a fast adiabatic passage through resonance [6]. Another way to make Bragg transitions robust with respect to parameter variations of light pulses is to numerically optimize the light pulses so that they can maintain an efficient momentum transfer even under substantial intensity fluctuations and frequency deviations [16]. It will be shown below that the momentum transfer that is robust to variations in the parameters of the atom–field interaction can also be realized using two pairs of counter-propagating light pulses with different detuning from the Bragg resonance in each of those pairs.

4.2. Bragg transitions under the action of four light pulses

Now let us consider Bragg transitions in an atom subjected to the action of four light pulses and show that if the parameters of the atom–field interaction vary within certain limits, the momentum transferred to the atom can be practically constant. The influence of parameter changes on the result of atom–field inter-

action will be illustrated for the quantities R_0, δ_0, δ, $t_{d1} - t_{d2}$ (we assume that pulses 1, 3, as well as pulses 2, 4 coincide in time in pairs), and τ (the durations of the light pulses are assumed to be identical).

The number of independent parameters was intentionally restricted to a minimally sufficient set, which allows us to demonstrate the robustness of Bragg transitions with respect to their variations without introducing excessive complexity. The extension of the analysis to the full set of parameters that characterize the light pulses and their interaction with the atom could potentially reveal new features of transitions in the four-pulse field. However, this is not a primary objective at the current stage of research.

4.2.1. Robustness of Bragg transitions to the variation in two-photon Rabi frequency

Figure 4 illustrates the robustness of the average momentum transferred to the atom with respect to the change of the quantity R_0, which is the scale for the time-dependent two-photon Rabi frequencies $\sqrt{R_1 R_3}$ and $\sqrt{R_2 R_4}$. For illustration, we have chosen Bragg transitions of the same order as in Fig. 3. The difference between the figures is that the two-photon detunings from resonance are different for different pairs, whereas the average two-photon detunings for the two-, four-, and six-photon transitions are the same as in Fig. 3. At the same time, the difference between the two-photon detunings is identical for all curves, $\delta = 10\delta_{\text{rec}}$, and has an order of magnitude as the average two-photon detuning δ_0. One can observe stable two-, four-, and eight-photon transitions; six-photon transitions are not observed here (they can be realized at other values of the atom–field interaction parameters), which testifies to the absence of a transition close to adiabatic in this case. It is noteworthy that in the curves with $\delta_0 = 4\delta_{\text{rec}}$ and $12\delta_{\text{rec}}$, which were calculated for two- and six-photon transitions, respectively, the four-photon transition is also observed (within a rather wide interval $5.3\delta_{\text{rec}} < R_0 < 6.68\delta_{\text{rec}}$), which indicates the formation of an adiabatic state coupling the states with zero atomic momentum and momentum $4\hbar k$. Thus, the intuitive requirement that the average two-photon detuning must be in resonance with the frequency of this transition for the formation of a Bragg transition is not always satisfied.

4.2.2. Robustness of Bragg transitions to the variation of the average two-photon detuning

Now let us consider the momentum transfer robustness to the change of the average two-photon detuning δ_0. The parameter values for illustrative calculations were chosen on the basis of Fig. 4. In order to illustrate the robustness of four-photon transition to the variation of the average two-photon detuning from resonance, we carried out calculations for $R_0 = 4\delta_{\text{rec}}$. In addition, we performed calculations for $R_0 = 10\delta_{\text{rec}}$, which allowed us to demonstrate the robustness of two- and eight-photon transitions to the variation of δ_0 near the resonance. The results of the calculations are shown in Fig. 5.

Besides the expected plateaus in the dependence of the momentum transferred to the atom near $\delta_0 = 8\delta_{\text{rec}}$ ($7.09\delta_{\text{rec}} < \delta_0 < 8.91\delta_{\text{rec}}$) and $\delta_0 = -8\delta_{\text{rec}}$ ($-8.36\delta_{\text{rec}} < \delta_0 < -7.63\delta_{\text{rec}}$, the change of the momentum transfer direction to the opposite), Fig. 5 also contains other intervals of δ_0-values, at which the momentum $\pm 4\hbar k$ is transferred to the atom with an insignificant sensitivity to the change of δ_0; these are the intervals $\delta_0 = [-12.95\delta_{\text{rec}}, -12.55\delta_{\text{rec}}]$, $[-3.45\delta_{\text{rec}}, -3.05\delta_{\text{rec}}]$, $[3.05\delta_{\text{rec}}, 3.42\delta_{\text{rec}}]$, and $[12.6\delta_{\text{rec}}, 12.95\delta_{\text{rec}}]$. The ends of the plateaus were determined based on the require-

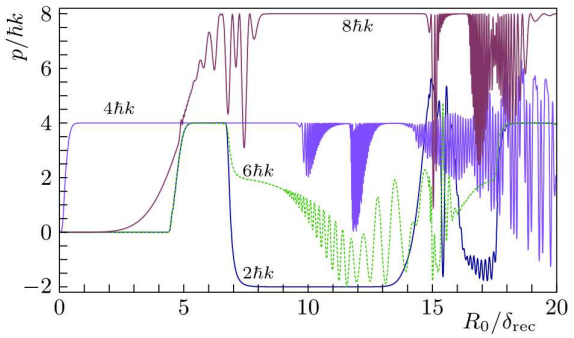

Fig. 4. Dependences of the average momentum transferred to the atom on the two-photon Rabi frequency. At the beginning of its interaction with the field, the atom is in a state with zero momentum. The differences between the two-photon detunings of pulse pairs 1–3 ($\delta_1 - \delta_3$) and 2–4 ($\delta_2 - \delta_4$) are identical for all curves and equal to $\delta = 10\delta_{\text{rec}}$; their average value corresponds to two- ($\delta_0 = 4\delta_{\text{rec}}$, curve $2\hbar k$), four- ($\delta_0 = 8\delta_{\text{rec}}$, curve $4\hbar k$), six- ($\delta_0 = 12\delta_{\text{rec}}$, curve $6\hbar k$), and eight-photon ($\delta_0 = 16\delta_{\text{rec}}$, curve $8\hbar k$) Bragg transitions. The durations of the light pulses are identical, $\tau = 400\pi/\delta_{\text{rec}}$. $t_{d1} = t_{d3} = 0.175$, $t_{d2} = t_{d4} = -0.175$, $\varphi = 0$

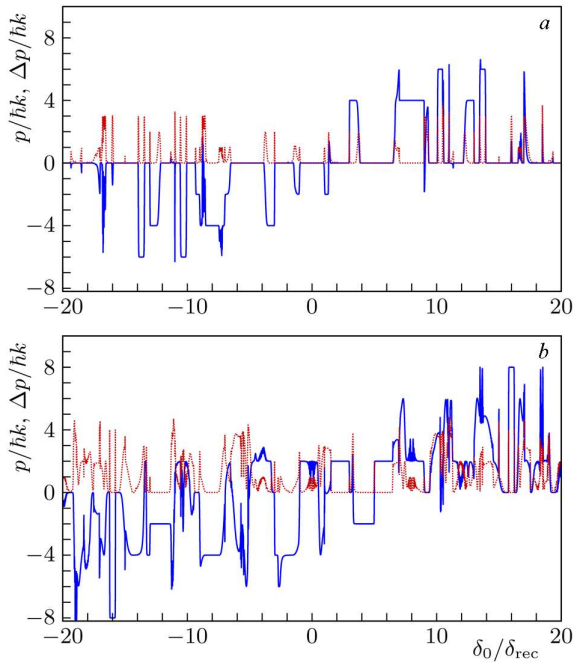

Fig. 5. Dependences of the average momentum transferred to the atom (solid curve) and the root-mean-square deviation of the transferred momentum from its average value (dashed curve) on the average detuning of the light pulses from the two-photon resonance. At the beginning of its interaction with the field, the atom is in a state with zero momentum. The durations of all pulses are identical, $\tau = 400\pi/\delta_{\rm rec}$, $t_{d1} = t_{d3} = 0.175$, $t_{d2} = t_{d4} = -0.175$. The difference between the two-photon detunings of pulse pairs 1–3 and 2–4 is $\delta = 10\delta_{\rm rec}$. $\varphi = 0$. $R_0 = 4\delta_{\rm rec}$ (a) and $10\delta_{\rm rec}$ (b)

ment that the root-mean-square deviation Δp of the momentum transferred to the atom from its average value p should not exceed $0.01\hbar k$ (dotted curves in Fig. 5).

As can be seen from Fig. 5, at $R_0 = 4\delta_{\rm rec}$, a momentum transfer of $2\hbar k$ ($1.10\delta_{\rm rec} < \delta_0 < 1.25\delta_{\rm rec}$) and $6\hbar k$ ($-13.81\delta_{\rm rec} < \delta_0 < 13.57\delta_{\rm rec}$) is also possible, which is far from the conditions for two- or six-photon resonance in the field of two counter-propagating waves. Thus, the tuning of the average two-photon detuning of the counter-propagating pulse pairs to a region near the corresponding multiphoton transition is not at all necessary for the formation of a Bragg transition that is robust to the variation of the atom–field interaction parameters. Furthermore, the corresponding multiphoton transition may not be observed at this tuning, as one can see in Figs. 4 and 5 for the case of the six-photon transition.

It is noteworthy that in the case of δ_0-tuning near $\mp 8\delta_{\rm rec}$, which corresponds to the four-photon Bragg transition in the case of the atom interaction with two light pulses, the plateau ends ($\pm 0.37\delta_{\rm rec}$ and $\pm 0.91\delta_{\rm rec}$) are symmetric with respect to this value, similarly to the case of atom interaction with two counter-propagating light pulses with different carrier frequencies [2]; the difference is that in the case of Bragg transition, the plateau boundaries are located not at $\pm\frac{1}{2}\delta$ but at a different distance relative to its center. At the same time, as marked above, near $8\delta_{\rm rec} \pm \frac{1}{2}\delta$ and $-8\delta_{\rm rec} \pm \frac{1}{2}\delta$ (these δ_0-values correspond to the resonance with the four-photon Bragg transition of either pairs of light pulses), small plateaus corresponding to the four-photon transition are observed. Similarly to Ref. [2], the root-mean-square deviations of the atomic momentum from its average value at these points are equal to the absolute value of the average transmitted momentum ($|p| = \Delta p = 2\hbar k$), which corresponds in our picture to the splitting of the atomic wave into two ones: with momenta $0\hbar k$ (the primary wave) and $4\hbar k$. As can be seen from the figure, such a splitting is also possible for other δ_0-values, for example, at $\delta_0 = 3.74\delta_{\rm rec}$; and the splitting of the atomic packet into packets with zero momentum and momentum $-6\hbar k$ is possible near $\delta_0 = -10.55\delta_{\rm rec}$. Thus, the analyzed scheme of the atom–field interaction can be used to split the atomic wave packet.

For a significantly larger Rabi frequency, up to $10\delta_{\rm rec}$ (Fig. 5, b), the robust transfer of the light momentum $4\hbar k$ to an atom occurs only within the interval $-8.48\delta_{\rm rec} < \delta_0 < -7.55\delta_{\rm rec}$. At the same time, there appear δ_0-intervals where the following momentum transfers are possible: $-2\hbar k$ in ($-12.94\delta_{\rm rec} < \delta_0 < -11.55\delta_{\rm rec}$) and ($3.65\delta_{\rm rec} < \delta_0 < 4.93\delta_{\rm rec}$), $2\hbar k$ in ($1.58\delta_{\rm rec} < \delta_0 < 2.94\delta_{\rm rec}$) and ($5.07\delta_{\rm rec} < \delta_0 < 6.4\delta_{\rm rec}$), and $8\hbar k$ in ($15.85\delta_{\rm rec} < \delta_0 < 16.15\delta_{\rm rec}$). At some δ_0-values, the atomic wave packet can be split into two packets. For example, at $\delta_0 = -16.23\delta_{\rm rec}$, after the atom has interacted with the field of light pulses, the initial wave packet with zero momentum splits into two ones: with momenta $0\hbar k$ and $-8\hbar k$. The splitting of the wave packet into two ones is observed neither at $\delta_0 = -8\delta_{\rm rec} \pm \frac{1}{2}\delta$ or $\delta_0 = 8\delta_{\rm rec} \pm \frac{1}{2}\delta$, nor at $\delta_0 = -16\delta_{\rm rec} + \frac{1}{2}\delta$ or $\delta_0 = 8\delta_{\rm rec} - \frac{1}{2}\delta$. Of course, the aforesaid is applicable only to the δ_0-dependences of the momentum transferred to the atom and its dispersion for the values

of the atom–field interaction parameters that correspond to Fig. 5, *b*.

In Fig. 5, one can also see regions corresponding to the return of the atom to its initial state after its interaction with the field (coherent population return, also an adiabatic process). In these regions, both the momentum transferred to the atom and its root-mean-square deviation from the average value are equal to zero.

4.2.3. Robustness of Bragg transitions to the variation of the difference δ of two-photon detunings of light pulses

Figure 6 illustrates the robustness of Bragg transitions to the variation of the difference δ of two-photon detunings of light pulse pairs 1–3 and 2–4. Panels *a* and *b* demonstrate the robustness of four-photon transitions for two-photon Rabi frequencies $R_0 = 4\delta_{\rm rec}$ and $10\delta_{\rm rec}$. In particular, they testify that a high Rabi frequency is not the best way to achieve the robustness of Bragg transitions. The δ-dependences of the average transferred momentum of the atom, p, and its root-mean-square deviation from the average value, Δp, depicted in panel *c* were calculated to verify whether it is possible, by changing δ provided $\delta_0 = 12\delta_{\rm rec}$ and $R_0 = 4\delta_{\rm rec}$, to find an interval for δ where the six-photon Bragg transition is robust to the change of this parameter. As one can see, no such interval was found. Instead, we found that by tuning δ_0 to the six-photon resonance region at the corresponding δ-values, we can obtain an eight-photon Bragg transition; see the intervals $[-18.92\delta_{\rm rec}, -18.45\delta_{\rm rec}]$ and $[16.15\delta_{\rm rec}, 18.92\delta_{\rm rec}]$ in Fig. 6, *c*. Figure 6, *c* also contains intervals where two-photon Bragg transitions that are robust to δ-variation can be observed.

Similarly to Fig. 5, the dependences shown in Fig. 6 have some features. Some of them can be predicted if we take into account that the atom is in the field of counter-propagating pulses with the carrier frequencies $\delta_0 \pm \frac{1}{2}\delta$. This means that one of the pairs of light pulses is in resonance with the two- ($\delta = \pm 8\delta_{\rm rec}$), four- ($\delta = 0$), six- ($\delta = \pm 8\delta_{\rm rec}$), and eight-photon ($\delta = \pm 16\delta_{\rm rec}$) Bragg transitions (Figs. 6, *a* and 6, *b*), as well as to the two- ($\delta = \pm 16\delta_{\rm rec}$), four- ($\delta = \pm 8\delta_{\rm rec}$), six- ($\delta = 0$), and eight-photon ($\delta = \pm 8\delta_{\rm rec}$) Bragg transitions (Fig. 6, *c*). The other features are probably associated with the non-adiabatic character of the atom–field interaction. This is illustrated in Fig. 7, where the dependences of the population of the states with momenta $2\hbar k$ (dashed curve) and $4\hbar k$ (solid curve) on the detuning difference δ for pulse pairs 1–3 and 2–4 from the two-photon resonance within the interval $10\delta_{\rm rec} < \delta < 12\delta_{\rm rec}$ are shown; this interval corresponds to the plateau and

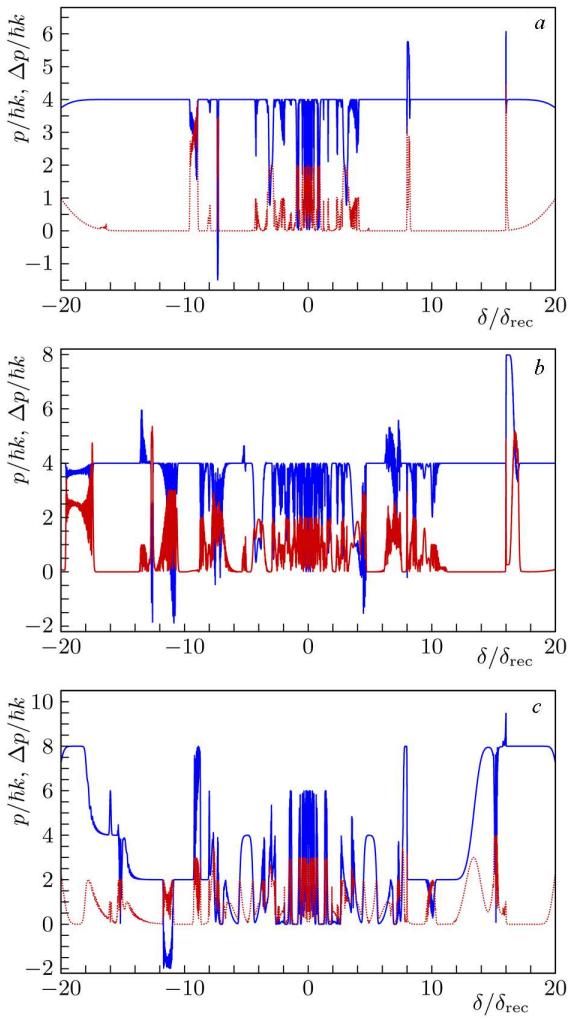

Fig. 6. Dependences of the average momentum transferred to the atom (solid curves) and the root-mean-square deviation of the transferred momentum from its average value (dashed curves) on the difference δ between the detunings of pulse pairs 1–3 and 2–4 from the two-photon resonance. At the beginning of its interaction with the field, the atom is in a state with zero momentum. The durations of all pulses are identical, $\tau = 400\pi/\delta_{\rm rec}$. $t_{d1} = t_{d3} = 0.175$, $t_{d2} = t_{d4} = -0.175$. The average two-photon detuning between pulse pairs 1–3 and 2–4 is $\delta_0 = 8\delta_{\rm rec}$ (*a*,*b*) and $12\delta_{\rm rec}$ (*c*). $R_0 = 4\delta_{\rm rec}$ (*a*) and $10\delta_{\rm rec}$ (*b*,*c*). $\varphi = 0$

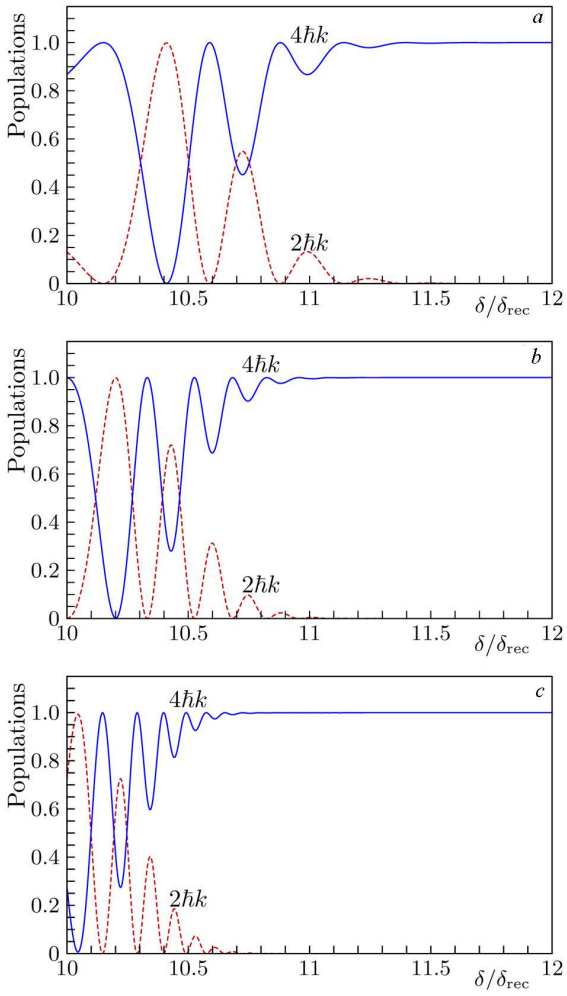

Fig. 7. Population dependences of states with momenta $4\hbar k$ (solid curve) and $2\hbar k$ (dashed curve) on the difference δ between the detunings of pulse pairs 1–3 and 2–4 from the two-photon resonance. At the beginning of its interaction with the field, the atom is in a state with zero momentum. The pulse durations are identical: $\tau = 100\pi/\delta_{\rm rec}$ (a), $200\pi/\delta_{\rm rec}$ (b), and $400\pi/\delta_{\rm rec}$ (c). The delay between the pulse pairs is 0.35τ ($t_{d1} = t_{d3} = 0.175$, $t_{d2} = t_{d4} = -0.175$). The average two-photon detuning between pulse pairs 1–3 and 2–4 is $\delta_0 = 8\delta_{\rm rec}$. $R_0 = 10\delta_{\rm rec}$; $\varphi = 0$

the region with oscillations near it in Fig. 6, *b*. As in the previous figures, the plots in Fig. 6 were calculated for the case $\varphi = 0$. For other φ-values, especially in the plateau regions and near them, the plots have the same appearance, at least up to seven decimal places, except for a very small set of parameters, where the dependence on φ can be observed, mainly at $|\delta| < \delta_{\rm rec}$.

Unlike Fig. 6, where the dependences of the average momentum and its standard deviation from the mean value are shown, Fig. 7 demonstrates the δ-dependences of population for states with a certain momentum value. Various panels correspond to various pulse durations: $\tau = 100\pi/\delta_{\rm rec}$ (a), $200\pi/\delta_{\rm rec}$ (b), and $400\pi/\delta_{\rm rec}$ (c). As one can see, near the plateau, the final state of the atom after its interaction with the field is a superposition of states with momenta $2\hbar k$ and $4\hbar k$; it oscillates as δ changes. Such a behavior of the populations of the pulsed states can be interpreted as follows. Changes in the parameters of the atom–field interaction – in particular, δ–lead to variations in the energies of the adiabatic states of the atom. If these energies are separated sufficiently far from each other, the atom is in one of the adiabatic states, which are associated with the state with zero momentum at the beginning of the atom–field interaction, and with the state with momentum $4\hbar k$ at the end of interaction. As δ changes, the eigenvalues of this adiabatic state approach, at certain time moments, the eigenvalues of the adiabatic state that corresponds to momentum $2\hbar k$ at the end of atom–field interaction. If their difference is large enough, the atom is in either adiabatic state. As the difference decreases, Landau–Zener transitions [17, 18] between the adiabatic states take place. The probability of these transitions increases as the time spent by the atom near the Landau–Zener transition decreases, i.e., as the pulse duration decreases. Indeed, from a comparison of panels in Fig. 7, one can see that as τ increases, the beginning of the plateau shifts towards smaller δ, i.e., the region of adiabatic atom–field interaction expands in accordance with the decrease of the probability of Landau–Zener transitions.

The presence of oscillations indicates the interference of the atomic packet components at the Landau–Zener transition. This means that the wave packet corresponding to the atom with zero momentum was split into two parts when the eigenvalues of the adiabatic states became closer to each other, and in time, when the next Landau–Zener transition was reached, each part was split into two parts, common to both adiabatic states, with the subsequent pair-wise interference of the components corresponding to momenta $4\hbar k$ and $2\hbar k$.

During the evolution of the atomic wave packet within the time interval in which the eigenvalues approach each other, each component of the superposi-

tion of two states acquires a certain phase. The phase difference between these states is of the order of

$$\Delta\varphi \approx \frac{S}{\hbar}\tau, \tag{24}$$

where S is the average difference between the eigenvalues of adiabatic states. It is this phase is responsible for the interference of the adiabatic atomic states. As one can see from Eq. (24), if the change in δ is small and the associated change of the difference between the eigenvalues of the adiabatic states is also small, the phase difference between the pulse components of the wave packet before the second approach of the eigenvalues and the splitting of each of them into two ones at the Landau–Zener transition can be substantial due to the large duration of light pulses. As a result, the distribution of the atoms over their momenta after the end of their interaction with the field becomes more sensitive to δ: as the pulse duration increases, the populations of states with momenta $2\hbar k$ and $4\hbar k$ oscillate more frequently (see Fig. 7).

From Fig. 7, we see that as a result of the atom–field interaction, we have a superposition of states with momenta $2\hbar k$ and $4\hbar k$ near the plateau, and atoms with momentum $4\hbar k$ on the plateau. This indicates that atoms in an adiabatic state close to the one that connects the state with zero momentum before the atom–field interaction with the state with momentum $4\hbar k$ should have momentum $2\hbar k$ after the interaction with the field. Numerical calculations show that, within the calculation accuracy, for the parameters corresponding to Fig. 7, *a*, but with an initial atomic momentum of $2\hbar k$, the δ-dependences of the populations of the state with momenta $2\hbar k$ and $4\hbar k$ have the same form if we replace $2\hbar k \leftrightarrow 4\hbar k$. Thus, when an atom in the initial state with zero momentum interacts with the field, at least for the set of parameters shown in Fig. 7, Landau–Zener transitions may occur between the adiabatic state that connects the state with zero momentum of the atom at the beginning of its interaction with the field with the state with momentum $4\hbar k$ after this interaction, and the adiabatic state that corresponds to momentum $2\hbar k$ both before and after the atom–field interaction. Whence it follows that for the initial atomic wave packet in the form of a superposition of states with momenta $0\hbar k$ and $2\hbar k$, the population of the momentum components of the final state will depend on the phase difference between the momentum components of the initial state, which can be used to determine the phase difference in atomic interferometers, as described earlier for the case of a two-level atom in the field of two counter-propagating light pulses [19].

According to the results presented above, as the duration of light pulses decreases, the plateaus' widths, which correspond to the robustness limits of the momentum transferred to the atom at Bragg scattering with respect to a particular parameter, also decrease. However, even at light pulse durations much shorter than those used in plotting Fig. 7, the plateau-like regions still remain in the dependences of the momentum transferred to the atom or the populations of momentum states on the parameters of interaction between the atoms and the field of light pulses. For example, for the parameters corresponding to Fig. 6, *a*, but with $\tau = 40\pi/\delta_{\text{rec}}$, the transfer of momentum $4\hbar k$ to the atom, which is robust to the δ-change, is possible within the intervals $-6.99\delta_{\text{rec}} < \delta < -5.72\delta_{\text{rec}}$ and $5.72\delta_{\text{rec}} < \delta < 7.66\delta_{\text{rec}}$, and the dependences of the momentum transferred to the atom and its standard deviation from the mean value, which are shown in Fig. 6, *b*, are close to their counterparts for the case $\tau = 100/\delta_{\text{rec}}$.

4.2.4. Robustness of Bragg transitions to the variation of the time delay between the pairs of light pulses

Another parameter that affects the momentum transfer to an atom at Bragg transitions is the time delay between the light pulses. Here we confine our consideration to the most natural case, when the pulses coincide in time pairwise providing a two-photon transition; in addition, the duration of all pulses is identical. In Fig. 8, it is shown how the average momentum transferred to the atom and its root-mean-square deviation from the average value change depending on the dimensionless time delay between the pulses. For all curves, the value $\delta = 10\delta_{\text{rec}}$ was chosen, and the value δ_0 was chosen so that it would correspond to two-, four-, six-, and eight-photon Bragg transitions in the case of two light pulses. The vertical dashed lines in Fig. 8 mark the delay between the pairs of light pulses; namely, $t_{d1} - t_{d2} = t_{d3} - t_{d4} = 0.35\tau$, for which the calculations were performed.

Figure 8 correlates with Fig. 5. Two- and eight-photon transitions are observed in both of them at

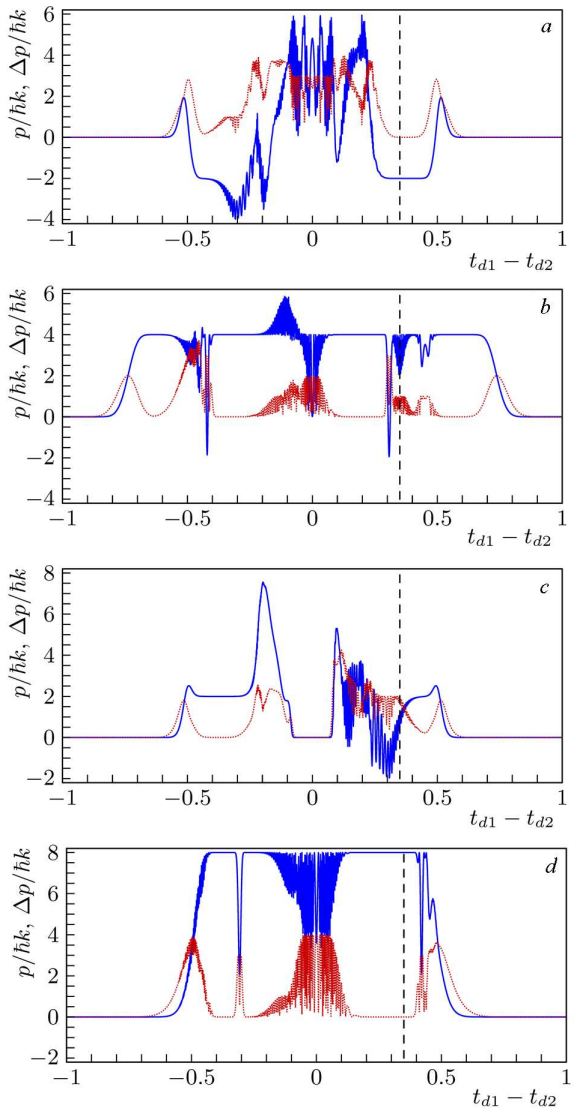

Fig. 8. Dependences of the average momentum transferred to the atom (solid curves) and the root-mean-square deviation of the transferred momentum from its average value (dashed curves) on the delay between the pulses. At the beginning of its interaction with the field, the atom is in a state with zero momentum. The durations of all pulses are identical, $\tau = 400\pi/\delta_{\text{rec}}$. The average two-photon detuning is $\delta_0 = 4\delta_{\text{rec}}$ (a), $8\delta_{\text{rec}}$ (b), $12\delta_{\text{rec}}$ (c), and $16\delta_{\text{rec}}$ (d). The difference between the two-photon detunings of pulse pairs 1–3 and 2–4 is $\delta = 10\delta_{\text{rec}}$; $\varphi = 0$. The maximum values of the two-photon Rabi frequencies are identical, $R_0 = 10\delta_{\text{rec}}$

a delay of 0.35τ between the pairs of pulses, whereas four- and six-photon transitions at such a delay are absent in both figures. At the same time, when the delay between the pairs of pulses is varied in either direction, four-photon transitions can be observed, but not six-photon ones (at the selected values $\delta = 10\delta_{\text{rec}}$ and $\delta_0 = 12\delta_{\text{rec}}$). This means that the variation of only one of the parameters describing the interaction of the atom with the field of light pulses may not be sufficient to realize a Bragg transition of the desired order, so an appropriate choice of the parameter set is necessary. For instance, the six-photon transition, as was indicated above, can be seen in Fig. 5, *a*.

We have illustrated the robustness of the transfer of a certain momentum to an atom at Bragg transitions in the field of two counter-propagating pairs of light pulses with respect to the variation in the atom–field interaction parameters. Now we will show how Bragg transitions can be used to split one atomic wave packet into two packets and as an atomic mirror that changes the momentum of an atom to the opposite direction.

4.2.5. Splitting of atomic wave packet

In Ref. [2], where the transfer of a mechanical momentum to an atom in the field of counter-propagating light pulses was studied, it was shown that the atomic packet is split in half if the carrier frequency of either of light pulses is resonant with the transition frequency in the atom. For Bragg transitions, an analogous splitting of the wave packet is possible if the frequency difference in either of the pairs of light pulses is resonant to the Bragg transition frequency. In addition, as was noted when describing Fig. 5, the splitting of the packet into two ones at Bragg transitions is also possible for other δ_0-values.

In Fig. 9, it is shown how the distribution of atomic wave packets over the momentum changes if the difference between the carrier frequencies in a pair of light pulses corresponds to the four-photon transition. Initially, the atom was in a state with zero momentum. As can be seen, for a larger set of δ-values within the interval from zero to $10\delta_{\text{rec}}$, as a result of interaction with the field, we have a splitting of the atomic wave packet into two packets: with zero momentum (as it was before the interaction) and momentum $4\hbar k$. In addition, in panel *a*, if the pair of pulses resonant with the Bragg transition interacts last with the atom, then at certain values of δ after the end of atom–field interaction, the atom can be in the state with momentum $2\hbar k$ and in narrow in-

tervals of states with zero momentum or momentum $4\hbar k$. In the opposite case, if the pair of pulses resonant to the Bragg transition interacts first with the field, then, besides the splitting of the atomic wave packet into two packets with zero momentum and momentum $4\hbar k$, it is possible, for a small set of δ-values, to split the atomic wave packet into two packets with zero momentum and momentum $2\hbar k$ or $-2\hbar k$, or two packets with momenta $2\hbar k$ and $4\hbar k$. Furthermore, for a small set of δ-values, the atom in the state with zero momentum or momentum $4\hbar k$ is a possible result of its interaction with the field.

Note that we have a peculiarity at $\delta = 8\delta_{\text{rec}}$, which is not visible in Fig. 9. In Fig. 9, *b*, the populations of the states with momenta $0\hbar k$ and $4\hbar k$ at this point ($\delta_0 = 4\delta_{\text{rec}}$, $\delta = 8\delta_{\text{rec}}$) are identical to five decimal places, 0.39747, but they differ noticeably from 0.5. In Fig. 9, *a*, the populations of the states with momenta $0\hbar k$ and $4\hbar k$ at this point ($\delta_0 = 12\delta_{\text{rec}}$, $\delta = 8\delta_{\text{rec}}$) are different: the population of the state with zero momentum equals 0.5 to five decimal places, and the population of the state with momentum $4\hbar k$ is only 0.39753. The reason is the resonant interaction of the atom with another pair of light pulses. In case *a*, this is the resonance with an eight-photon Bragg transition ($\delta_2 - \delta_4 = 16\delta_{\text{rec}}$), and the change of the atomic momentum by $8\hbar k$; in case *b*, the carrier frequencies of the first and third pulses are identical, which corresponds to a Bragg resonance for the transition between the states with momenta $4\hbar k$ and $-4\hbar k$.

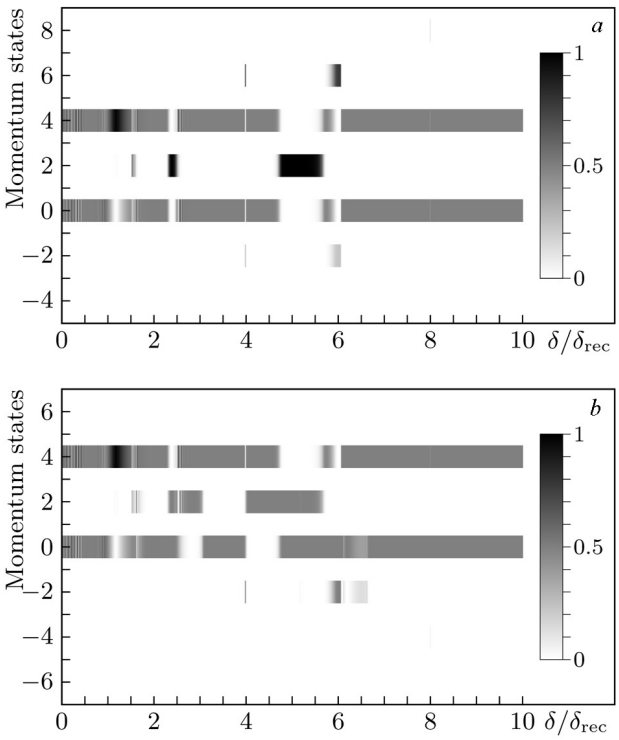

Fig. 9. Dependences of the final populations of states with various momenta on the difference δ between two-photon detunings in light pulse pairs 1–3 and 2–4 in the cases when (*a*) the first ($\delta_1 - \delta_3 = \delta_0 - \frac{1}{2}\delta = 8\delta_{\text{rec}}$) or (*b*) the second ($\delta_2 - \delta_4 = \delta_0 + \frac{1}{2}\delta = 8\delta_{\text{rec}}$) of those pairs is in resonance with the Bragg transition from the state of the atom with zero momentum to the state with momentum $4\hbar k$. The durations of all pulses are identical, $\tau = 400\pi/\delta_{\text{rec}}$. $R_0 = 3\delta_{\text{rec}}$, $t_{d1} = t_{d3} = 0.175$, $t_{d2} = t_{d4} = -0.175$, $\varphi = 0$

4.2.6. Atomic mirror

So far we have considered the case where the atom has a zero momentum component along the propagation direction of light pulses before its interaction with the field. Among all the cases with non-zero components of the atomic momentum along this direction, we are especially interested in those where the momentum changes to the opposite after the atom–field interaction, i.e., the light pulses serve as a mirror for atoms. In the case of two counter-propagating light pulses with identical carrier frequencies, we have Rabi oscillations, when the populations of the initial and final atomic states depend on the laser radiation intensity and the duration of light pulses. Let us demonstrate the possibility of a total repulsion of atoms by the field of two pairs of counter-propagating pulses, which is robust to the changes in the parameters of light pulses. Intuitively, one might expect such repulsion to occur at zero average two-photon detuning, $\delta_0 = 0$. In reality, this may or may not be the case because we had not always a certain Bragg transition for the corresponding δ_0. For example, we had a certain Bragg transition at $\delta_0 = 12\delta_{\text{rec}}$, but there is no such a six-photon transition in Fig. 5. At the same time, this six-photon transition can be observed Fig. 5 at other δ_0-values.

Figure 10 demonstrates the dependences of the populations of the states with different momenta of the atom after its interaction with two pairs of counter-propagating pulses on the maximum two-photon Rabi frequency R_0. The differences between the two-photon detunings in pairs 1–3 and 2–4 of light

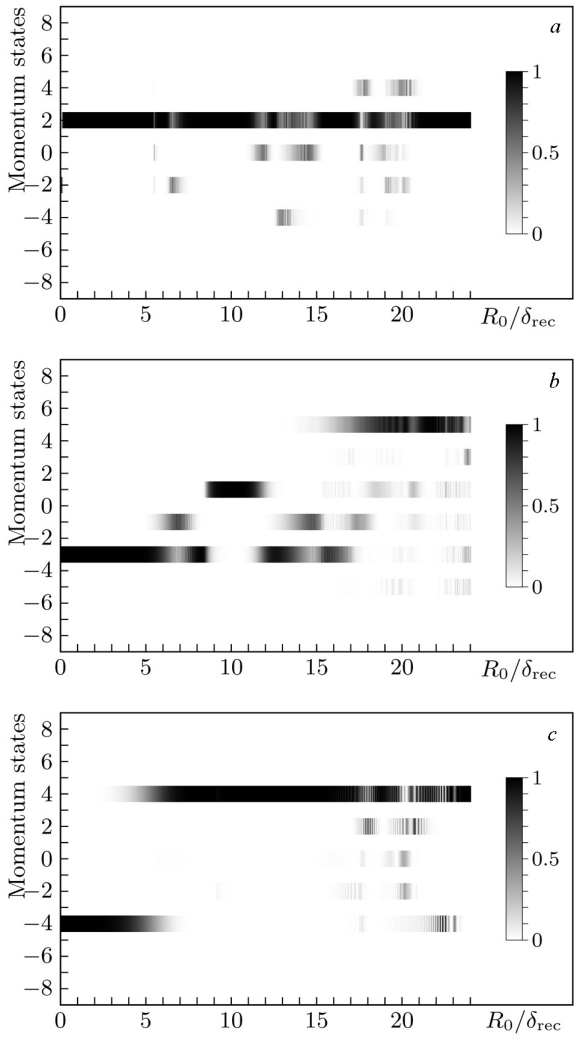

Fig. 10. Dependences of the final populations of states with various momenta on the maximum value R_0 of two-photon Rabi frequencies $\sqrt{R_1R_3}$ and $\sqrt{R_2R_4}$ for the average two-photon detuning $\delta_0 = 0$ of light pulse pairs in the cases when the initial momentum of the atom equals $-2\hbar k$ (a), $-3\hbar k$ (b), and $-4\hbar k$ (c). The duration of the light pulses is $\tau = 400\pi/\delta_{\rm rec}$, the difference between the two-photon detunings in the pulse pairs is $\delta = 5\delta_{\rm rec}$, $t_{d1} = t_{d3} = 0.175$, $t_{d2} = t_{d4} = -0.175$

pulses are $\delta = 5\delta_{\rm rec}$, and the average two-photon detuning is $\delta_0 = 0$. As we can see from the figure, there exists an interval of R_0-values where the field of the pulses serves as a mirror for atoms with the initial momenta of both $-2\hbar k$ (four-photon transition) and $-4\hbar k$. At the same time, a mirror for atoms with momentum $-3\hbar k$ is not realized within the entire interval of R_0-values. Instead, we have inelastic repulsion of such atoms with resulting momentum $1\hbar k$ (four-photon transition) in the interval $9.522\delta_{\rm rec} < R_0 < 10.824\delta_{\rm rec}$ (at a level of 0.99 and higher), and with resulting momentum $5\hbar k$ (eight-photon transition) in the interval $21.84\delta_{\rm rec} < R_0 < 21.90\delta_{\rm rec}$ (at a level of 0.99 and higher).

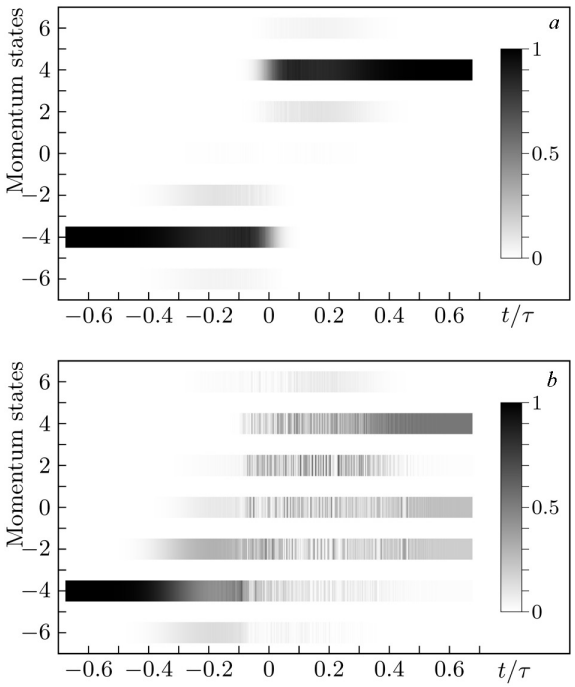

Fig. 11. Time dependences of the populations of the atomic states with various momenta for $R_0 = 10\delta_{\rm rec}$ (a) and $20\delta_{\rm rec}$ (b). The initial momentum of the atom is $-4\hbar k$, $\delta = 5\delta_{\rm rec}$, $\delta_0 = 0$, $\tau = 400\pi/\delta_{\rm rec}$, $t_{d1} = t_{d3} = 0.175$, $t_{d2} = t_{d4} = -0.175$

In Fig. 11, it is shown how the momentum distribution of the atomic wave packet changes in time in the cases (a) where a 100% specular reflection (robust to the variation of R_0) of the atomic wave packet by the field of two pairs of counter-propagating pulses takes place and (b) where there is no such reflection. The calculation parameters correspond to Fig. 10, c for $R_0 = 10\delta_{\rm rec}$ (Fig. 11, a) and $20\delta_{\rm rec}$ (Fig. 11, b). In Fig. 11, a, the behavior of the populations in time fully corresponds to the general picture of an adiabatic process, when the adiabatic state corresponds to the state of the atom with a certain momentum at the beginning and the end of the atom–field interaction, and to a superposition of states with different momenta during such interaction. Fi-

gure 11, *b* testifies that the atom–field interaction is non-adiabatic in this case.

4.2.7. Estimation of pulse duration and laser radiation intensity

a. Rubidium. Let us consider the transition $5^2S_{1/2} \rightarrow 5^2P_{3/2}$ in ^{85}Rb with the wavelength $\lambda = 780.24$ nm. The spontaneous emission lifetime is $\tau_{sp} = 26.63$ ns, the spontaneous emission rate is $\gamma/2\pi = 5.98$ MHz, $\delta_{rec} = \hbar k^2/(2M) = 2\pi \times 3.86$ kHz, and the intensity of transition saturation is $I_{sat} = 1.64$ mW/cm^2 [20].

According to Eq. (15), at $R_0 \approx 10\delta_{rec} = 2\pi \times 38.6$ kHz and $\Delta_{13} = 2\pi \times 50$ GHz, we have $\Omega_{10} = 2\pi \times 62$ MHz. Then, Eq. (11) gives an estimate for the maximum population of the excited state, $|b_{e,n}^{(1,3)}|^2 \approx 3.9 \times 10^{-7}$. For the pulse duration $\tau = 100\pi/\delta_{rec} = 13$ ms, criterion (10) yields $0.18 \ll 1$. To strengthen it, the intensity of light pulses and the detuning Δ_{13} from the resonance should be increased. Based on the relation

$$\Omega_{10} = \frac{1}{\tau_{sp}} \sqrt{\frac{I}{2I_{sat}}} \tag{25}$$

between the laser radiation intensity and the Rabi frequency, we obtain the laser radiation intensity at the pulse maximum, $I = 2I_{sat}(\Omega_{10}\tau_{sp})^2 = 0.35$ W/cm^2.

b. Strontium. Let us consider the weak intercombination transition $^1S_0 \rightarrow {}^3P_1$ in ^{88}Sr with the wavelength $\lambda = 689$ nm. The spontaneous emission lifetime is $\tau_{sp} = 21.6$ μs, the spontaneous emission rate is $\gamma/2\pi = 7.4$ kHz, $\delta_{rec} = \hbar k^2/(2M) = 2\pi \times 4.7$ kHz, and the intensity of transition saturation is $I_{sat} = 3$ μW/cm^2 [21–23].

According to Eq. (15), at $R_0 \approx 10\delta_{rec} = 2\pi \times 47$ kHz and $\Delta_{13} = 2\pi \times 500$ MHz, we have $\Omega_{10} = 2\pi \times 6.8$ MHz. Then, Eq. (11) gives an estimate for the maximum population of the excited state, $|b_{e,n}^{(1,3)}|^2 \approx 4.7 \times 10^{-5}$. If the pulse duration $\tau = 100\pi/\delta_{rec} = 10$ ms, criterion (10) yields $0.023 \ll 1$. To strengthen it, the intensity of light pulses and the detuning Δ_{13} from the resonance should be increased. Based on relationship (25) between the intensity of laser radiation and the Rabi frequency, we obtain the intensity of laser radiation at the pulse maximum, $I = 2I_{sat}(\Omega_{10}\tau_{sp})^2 = 5.2$ W/cm^2.

5. Conclusions

The present study demonstrates the robustness of Bragg transitions to the variation of the parameters describing the interaction of an atom with the field of two pairs of counter-propagating light pulses with different carrier frequencies. The main conclusions are as follows.

• The lower limit for the duration of light pulses, at which Bragg transitions remain robust to the variation of the parameters of light pulses can still be observed, can be estimated as a value of the order of 40–$100\,\delta_{rec}^{-1}$.

• We cannot state that the higher intensities of laser light pulses in Bragg transitions always expand the possibilities of the momentum transfer to an atom, which is robust to the variations of the atom–field interaction parameters.

• Provided a proper tuning of the carrier frequencies of the light pulses with respect to the Bragg resonance, it is possible to split a monochromatic atomic wave packet into two components with different momenta, but identical amplitudes.

• A mirror for atoms, implemented on the basis of their interaction with the field of two pairs of counter-propagating light pulses with different carrier frequencies, can provide an almost 100% momentum-selective specular repulsion, provided a proper choice of the atom–field interaction parameters.

• A comparison between the numerical estimates of the intensity of laser pulses and their duration obtained for Bragg transitions in rubidium and strontium (a weak intercombination transition) shows that for similar requirements to the two-photon Rabi frequency, the losses on spontaneous emission are approximately an order of magnitude lower and the required laser radiation intensity is an order of magnitude higher at the intercombination transition. At the same time, in order to implement Bragg transitions in the field of counter-propagating pairs of light waves, the detuning from the single-photon resonance can be two orders of magnitude lower.

Thus, the interaction of an atom with the field of two pairs of counter-propagating pulses with different carrier frequencies is an additional method for controlling atomic motion. It can provide both the transfer of a given momentum to an atom, which is robust to the variation of the atom–field interaction parameters, and, on this basis, the implementation of

such necessary tools in atomic optics as atomic wave packet splitters and selective laser mirrors.

This work was carried out within the framework of the project No. 1.4.B/210 "Generation of highly coherent laser fields, development of methods and means to control their characteristics, and research of quantum effects at the interaction of atoms, molecules, nano- and microparticles with laser fields with controlled parameters" of the National Academy of Sciences of Ukraine.

1. L. Allen, J.H. Eberly. *Optical Resonance and Two- Level Atoms* (John Wiley and Sons, 1975).
2. V.I. Romanenko, L.P. Yatsenko. Scattering of atoms in a bichromatic field of oppositely propagating light pulses. *J. Experimental and Theor. Phys.* **90**, 407 (2000).
3. G. Demeter, G.P. Djotyan, Z. Sörlei, J.S. Bakos. Mechanical effect of retroreflected frequency chirped laser pulses on two-lovel atoms. *Phys. Rev. A* **74**, 013401 (2006).
4. V.I. Romanenko, L.P. Yatsenko. Coherent momentum transfer due to interaction between three-level atoms and counterpropagating laser pulses. *J. Experimental and Theor. Phys.* **100**, 242 (2005).
5. D.M. Giltner, R.W. McGowan, S.A. Lee. Theoretical and experimental study of the Bragg scattering light wave. *Phys. Rev. A* **52**, 3966 (1995).
6. T. Kovachy, S.-w. Chiow, M.A. Kasevich. Adiabatic-rapid-passage multiphoton Bragg atom optics. *Phys. Rev. A* **86**, 011606 (2012),
7. J. Dalibard, Y. Castin, K. Mølmer. Wave-function approach to dissipative processes in quantum optics. *Phys. Rev. Lett.* **68**, 580 (1992).
8. K. Mølmer, Y. Castin, J. Dalibard. Monte Carlo wave-function method in quantum optics. *JOSA B* **10**, 524 (1993).
9. B. Shore. *The Theory of Coherent Atomic Excitation*, Vol. 1 (Wiley, 1990).
10. V.I. Romanenko. Stimulated Raman adiabatic passage in phase-fluctuating fields. *Ukr. J. Phys.* **51**, 1054 (2006).
11. S. Guérin, L.P. Yatsenko, H.R. Jauslin. Dynamical resonances and the topology of the multiphoton adiabatic passage. *Phys. Rev. A* **63**, 031403 (2001).
12. S. Guérin, H.R. Jauslin. *Control of Quantum Dynamics by Laser Pulses: Adiabatic Floquet Theory* (John Wiley & Sons, Ltd, 2003) [ISBN: 9780471428022].
13. L.P. Yatsenko, B.W. Shore, N.V. Vitanov, K. Bergmann. Retroreflection-induced bichromatic adiabatic passage. *Phys. Rev. A* **68**, 043405 (2003).
14. G. Demeter, G.P. Djotyan. Multiphoton adiabatic passage for atom optics applications. *J. Opt. Soc. Am. B* **26**, 867 (2009).
15. K. Varga-Umbrich, J.S. Bakos, G.P. Djotyan, Z. Sörlei, G. Demeter, P.N. Ignácz, B. Ráczkevi, J. Szigeti, M.A. Kedves. Coherent manipulation of trapped Rb atoms by overlapping frequency-chirped laser pulses: Theory and experiment. *Europ. Phys. J. D* **76**, 70 (2022).
16. G. Louie, Z. Chen, T. Deshpande, T. Kovachy. Robust atom optics for Bragg atom interferometry. *New J. Phys.* **25**, 083017 (2023).
17. L.D. Landau. Zur Theorie der Energieübertragung II. *Physikalische Zeitschrift der Sowjetunion* **2**, 46 (1932).
18. C. Zener. Non-adiabatic crossing of energy levels. In: *Proc. of the Royal Society of London. Series A* **137**, 696 (1932).
19. V.I. Romanenko, N.V. Kornilovska, L.P. Yatsenko. Controlling atomic wave interference by counter-propagating light pulses of different carrier frequencies. *Europ. Phys. J. D* **79**, 9 (2025).
20. H.J. Metcalf, P. van der Straten. *Laser Cooling and Trapping, Graduate Texts in Contemporary Physics* (Springer, 1999) [ISBN: 978-0-387-98747-7, 978-0-387-98728-6].
21. H. Katori, T. Ido, Y. Isoya, M. Kuwata-Gonokami. Magneto-optical trapping and cooling of strontium atoms down to the photon recoil temperature. *Phys. Rev. Lett.* **82**, 1116 (1999).
22. T. Ido, Y. Isoya, H. Katori. Optical-dipole trapping of Sr atoms at a high phase-space density. *Phys. Rev. A* **61**, 061403(R) (2000).
23. A.D. Ludlow, M.M. Boyd, J. Ye, E. Peik, P.O. Schmidt. Optical atomic clocks. *Rev. Mod. Phys.* **87**, 637 (2015).

Received 22.12.25
Translated from Ukrainian by O.I. Voitenko

В.І. Романенко, Л.П. Яценко

БРЕГГІВСЬКЕ РОЗСІЮВАННЯ АТОМІВ ЗУСТРІЧНИМИ СВІТЛОВИМИ ІМПУЛЬСАМИ, СТІЙКЕ ДО ЗМІНИ ЇХНЬОЇ ПЛОЩІ

Метою роботи є теоретичне дослідження бреггівських переходів дворівневого атома у полі двох пар зустрічних світлових імпульсів із різними несучими частотами. Бреггівські переходи розглядаються як когерентні мультифотонні процеси дифракції, у яких за належного налаштування на бреггівський резонанс імпульс атома може змінюватися на $2n\hbar k$ за один акт розсіювання, тоді як однофотонні переходи пригнічені через велику розладнаність відносно резонансу. Показано, що за такої конфігурації ефективність переходу практично не залежить від площі імпульсів, що відрізняє її від випадку однієї пари імпульсів. Фізичною основою цього ефекту є майже адіабатична взаємодія атома з полем, подібна до взаємодії з перекривними у часі зустрічними імпульсами з нерезонансними несучими частотами (В.І. Романенко, Л.П. Яценко, ЖЭТФ, 2000, Т. 117, № 3, с. 467–475; V.I. Romanenko and L.P. Yatsenko, JETP, T. 90, № 3, 2000, pp. 407–414). Також показано можливість стійкого до зміни інтенсивності розщеплення атомного пучка та формування селективних лазерних дзеркал. Запропонований підхід до керування рухом атомів може бути застосований для дослідження інтерференційних явищ в атомній оптиці.

Ключові слова: атомна оптика, лазерне випромінювання, бреггівський перехід, світловий тиск.